Research Article

Downregulation of ABLIM3 confers to the metastasis of neuroblastoma via regulating the cell adhesion molecules pathway

Baocheng Gong [a,1], Tongyuan Qu [a,b,1], Jiaojiao Zhang [b], Yubin Jia [a], Zian Song [a], Chong Chen [c], Jiaxing Yang [a], Chaoyu Wang [a], Yun Liu [b], Yan Jin [a,*], Wenfeng Cao [b,**], Qiang Zhao [a,*]

[a] Department of Pediatric Oncology, Tianjin Medical University Cancer Institute and Hospital, National Clinical Research Center for Cancer, Tianjin's Clinical Research Center for Cancer, Tianjin, China
[b] Department of Pathology, Tianjin Medical University Cancer Institute and Hospital, National Clinical Research Center for Cancer, Tianjin's Clinical Research Center for Cancer, Tianjin, China
[c] Department of Clinical Laboratory, Tianjin Medical University Cancer Institute and Hospital, Tianjin, China

ARTICLE INFO

ABSTRACT

Neuroblastoma (NB) is the most prevalent extracranial solid tumor in pediatric patients, and its treatment failure often associated with metastasis. In this study, LASSO, SVM-RFE, and random forest tree algorithms, was used to identify the pivotal gene involved in NB metastasis. NB cell lines (SK-N-AS and SK-N-BE2), in conjunction with NB tissue were used for further study. ABLIM3 was identified as the hub gene and can be an independent prognostic factor for patients with NB. The immunohistochemical analysis revealed that ABLIM3 is negatively correlated with the metastasis of NB. Patients with low expression of ABLIM3 had a poor prognosis. High ABLIM3 expression correlated with APC co-stimulation and Type1 IFN response, and TIDE analysis indicated that patients with low ABLIM3 expression exhibited enhanced responses to immunotherapy. Downregulation of ABLIM3 by shRNA transfection increased the migration and invasion ability of NB cells. Gene Set Enrichment Analysis (GSEA) revealed that genes associated with ABLIM3 were primarily enriched in the cell adhesion molecules (CAMs) pathway. RT-qPCR and western blot analyses demonstrated that downregulation of ABLIM3 led to decreased expression of ITGA3, ITGA8, and KRT19, the key components of CAMs. This study indicated that ABLIM3 can be an independent prognostic factor for NB patients, and CAMs may mediate the effect of ABLIM3 on the metastasis of NB, suggesting that ABLIM3 is a potential therapeutic target for NB metastasis, which provides a novel strategy for future research and treatment strategies for NB patients.

1. Introduction

Neuroblastoma (NB) stands as the most prevalent extracranial solid tumor affecting children in their early years, exhibiting an incidence rate of approximately 25–30 patients per million individuals [1–3]. Despite its relatively low incidence, NB contributes significantly to childhood cancer-related mortality, accounting for roughly 15 % of such fatalities [4]. NB is notable by its wide spectrum of clinical behaviors, including

spontaneous regression and favorable response to chemotherapy in patients younger than 18 months. However, approximately half of NB patients are diagnosed at an advanced stage, where they do not respond well to conventional chemotherapy and self-stem cell transplantation. The overall survival rate of these high-risk NB patients is reported to be less than 40 % [2,5]. Distant metastases with progressive have become a major obstacle in treating patients with NB, especially for high-risk patients, resulting in poor prognosis. This highlights the urgency to

identify a new potential key regulator of metastasis in NB.

While many studies have focused on exploring biomarkers associated with tumor metastasis [6], few have been used in clinical practice. Moreover, most biomarkers are mainly focused on early diagnosis and are rarely used for distant metastasis. With the advancement of sequencing technology, artificial intelligence, and machine learning significant progress has been made in the diagnosis and treatment of cancer [7–10]. To date, promising biomarkers with high sensitivity and specificity are still needed in clinical practice to diagnosis of NB metastasis, which is critical for identifying the key regulator in the process of NB metastasis.

The Actin Binding LIM Protein Family Member (ABLIM) has 3 subtypes, including ABLIM1/2/3, which mainly mediate the interactions between cytoplasmic targets and actin filaments and play a vital role in the formation of the cytoskeleton [11]. Previous research has shown that ABLIM1 could inhibit the progression of glioblastoma, and the phosphorylation of ABLIM1 mediates the role of Rictor in controlling actin polymerization in HCC cells [12,13]. Additionally, a decline in ABLIM2 expression has been observed in brain metastases originating from lung cancer, and the suppression of ABLIM2 has been identified as a mechanism that disrupts actin formation [14]. ABLIM3 plays a role in embryonic development, cell lineage determination, and progression of cancers [15]. Furthermore, ABLIM3 was identified as a newfound constituent of adherens junctions, displaying actin-binding capabilities [11]. Adherens junctions were reported to regulate epithelial integrity [16], and the structure destruction of adherens junction via E-cadherin expression attenuation, which increased intestinal epithelial permeability and diminished the function epithelial barrier [17]. In this study, based on the integrated machine learning analysis, ABLIM3 was identified as the key regulator in NB metastasis, but the role of ABLIM3 in the metastasis of neuroblastoma remains unclear.

The process of tumor metastasis is generally divided into four essential steps: detachment, migration, invasion, and adhesion, and is regulated by various signaling pathways and is affected by the surrounding extracellular matrix (ECM) [18,19]. Cell adhesion molecules (CAMs) are a large family of cell surface proteins, including the cadherin family, integrin (ITG) family, selectin family, immunoglobulin superfamily, and so on [20], which mediate attractive or repulsive forces to the ECM, stroma, and other cancer cells, and regulate cellular motility. CAMs play a very important role in cancer metastasis. Cadherin family members play a role in cancer metastasis by regulating epithelial-to-mesenchymal transition (EMT) [21]. Integrins can directly control the migration and invasion of cancer cells by binding to ECM components and establishing traction for cellular motility and invasion [22]. Selectins mainly promote metastasis by facilitating heterotypic interactions between cancer cells and blood components including endothelial cells [23], but the influence of ABLIM3 on the CAMs pathway was unclear.

In this research, a combination of machine learning algorithms and bioinformatic methodologies was employed to identify potential biomarkers for NB metastasis with functional relevance. Through this meticulous process, ABLIM3 was pinpointed as a significant marker. The multi-Cox regression analysis confirmed that ABLIM3 was an independent prognostic factor, positively associated with the Clinicopathological characteristics. Patients with high expression of ABLIM3 had a lower rate of tumor progression and active immune microenvironment. Downregulation of ABLIM3 enhances the migration and invasion ability of SK-N-AS and SK-N-BE2 cells by suppressing cell adhesion molecules ITGA3, ITGA8, and KRT19, with phalloidin staining showing increased formation of pseudopod. These results suggest that ABLIM3 is a promising biomarker for NB metastasis and a therapeutic target for NB patients.

2. Materials and methods

2.1. Data processing and differentially expressed gene identification

To identify the differentially expressed genes (DEGs) associated with metastasis in neuroblastoma, the RNA-seq data of neuroblastoma samples (9 localized NB tissues and 29 distant metastasis tissues) was downloaded from NCBI GEO database (GSE25624). Then, the "limma" package [24] was utilized to explore the DEGs between neuroblastoma in situ and metastasis sites in R software (Version 4.1.3). Those genes with $|\log 2FC| \geq 1$ and FDR < 0.05 were screened out as DEGs.

2.2. The potential signal pathway enrichment analysis

To investigate the potential mechanism of ABLIM3 in the metastasis of NB, we conducted the Gene ontology (GO) including biological process, Cellular Component, and Molecular Function, and Kyoto encyclopedia of genes and genomes (KEGG) pathway enrichment analysis. The background genes were accessed from "org.Hs.eg.db" in R software, and the DEGs were mapped. Then, biological processes and pathway enrichment analysis were conducted via the "clusterProfiler" in R software (Version 4.1.3) [25]. FDR < 0.05 were considered as statistically significant.

2.3. Integrated machine learning algorithms for differentially expressed genes

To identify the hub genes implicated in neuroblastoma metastasis, an analysis utilizing the Least Absolute Shrinkage and Selection Operator (LASSO) regression was conducted on the DEGs using the "glmnet" package in R software(Version 4.1.3) to avoid overfitting [26]. At the same time, the support vector machine-recursive feature elimination (SVM-RFE), which could remove the redundant factors and retain only variables related to metastasis [27], was conducted to identify the most optimal number of genes. Besides, the random forest algorithm, which is suitable for analyzing the importance of genes, was conducted to identify the most important gene that participates in the metastasis of NB patients [28].

2.4. The immune cell infiltration in neuroblastoma

To identify the different types of immune cells infiltrated in neuroblastoma, the "CIBERSORT" algorithm based on 22 different types of immune cells was conducted [29]. $P < 0.05$ was set as the threshold. Besides, the relative immune cell in tumors was compared between the localized neuroblastoma and metastasis site, and the comparisons were visualized with the "vioplot" package. Then the Tumor Immune Dysfunction and Exclusion (TIDE: http://tide.dfci.harvard.edu/ (accessed on August 15, 2023)) algorithms were performed to investigate the effectiveness of immunotherapy. Finally, the relationship between ABLIM3 expression and immune cells was analyzed using Spearman's rank correlation and visualized with the "ggpubr" package in R software (Version 4.1.3).

2.5. Potential sensitive drug exploration

The pharmacological responsiveness information was procured from the Genomics of Drug Sensitivity in Cancer (GDSC) database [30]. Chemotherapeutic response to potential drugs was quantified using the half-maximal inhibitory concentration (IC50), with the smaller the IC50 values indicating the stronger the sensitivity to specific compounds. Then, the relationship between the expression of ABLIM3 and different drugs was analyzed via the "pRRophetic" package in R software (Version 4.1.3). $P < 0.05$ was statistically significant.

2.6. Cell culture

The SK-N-AS and SK-N-BE2 cells used in this research were bought from the ATCC official website (https://www.atcc.org/, USA). These two kinds of cells were cultured in RPMI 1640 medium (Bionind, Israel), and incubated at a constant temperature of 37 °C in an atmosphere containing 5 % CO2. This medium was supplemented with 10 % fetal bovine serum (FBS, Bionind, Israel), 2 mM glutamine, and antibiotics including 1 % penicillin (100 units/mL) and 1 % streptomycin (100 μg/mL).

2.7. Cell transfection

The SK-N-AS and SK-N-BE2 cells were seeded into 6-well plates at a density of 2×10^5/well. After the cell reached about 60–70 % confluence, the ABLIM3 shRNAs were transfected into NB cells via JetPRIME reagents (Polyplus Transfection, Illkirsch, France). 8 h later, a new 1640 media will be used for further treatment. The sequences of short hairpin RNAs (ABLIM3 shRNAs and control shRNA) as following: ABLIM3 shRNA#1: GCCCACGTCATCGAGATATTT; shRNA#2: TCTACT-GAAGCTCGGTATAAT; shRNA#3: GTGGATAATGAGATCCTTAAT; Control shRNA: CCTAAGGTTAAGTCGCCCTCG.

2.8. Cell scratch assay

The SK-N-AS and SK-N-BE2 cells, following transfection with ABLIM3 shRNAs, were plated into 6-well plates at a density of 3×10^5 cells per well and incubated for 48 h in the incubation chamber. When the cell density reached 90 %, a pipette tip(200 μl) was used to scratch wounds. The 6-well plates were then washed with PBS (room temperature) 3 times to clear the detached cells, and then cells in the 6-well plates were incubated with fresh serum-free medium. The 6-well plates were visualized via the phase-contrast microscope (Olympus CKX53, Japan) at 0 h and 48 h. Finally, the percentage of distance was calculated by using ImageJ (Version 1.46).

2.9. Boyden chamber invasion assay

The SK-N-AS and SK-N-BE2 cells transfected with ABLIM3 shRNAs (5×10^4 cells/well), underwent serum deprivation for 8 h before being placed in the upper chambers of Transwell inserts. These inserts were pre-coated with Matrigel (2.5 mg/mL, BD Biosciences) and set within RPMI-1640 medium. The lower chambers were incubated with 800ul normal complete RPMI-1640 medium, and 48 h later, those non-invaded cells were removed from the upper chambers via cotton swabs. Subsequently, the cells that had invaded through the membrane were stained with crystal violet. The quantification was achieved by counting the cells in three randomly selected fields on each filter, utilizing a multiwell spectrophotometer for the analysis (BioTek, VT, USA).

2.10. Phalloidin staining

The SK-N-AS and SK-N-BE2 cells transfected with ABLIM3 shRNAs were cultured, 24 h later, and 4 % formalin was used to fix them for 20 min, and washed with phosphate-buffered saline (PBS) 3 times. NB cells were subsequently incubated in a solution containing 5 μg/mL of phalloidin conjugate (Sigma, CA, USA) diluted in PBS at a temperature of 37 °C for 40 min. Finally, to remove the unbound phalloidin conjugate, NB cells were washed with PBS (3 times/5 min), and fluorescence microscopy was used to display the images (Olympus, Tokyo, Japan), and Quantitation of F-actin was performed based on fluorescence intensity per area, n = 3 for each group, and Student's t test (two-tailed unpaired) was used for statistics.

2.11. Immunohistochemical (IHC) analysis

A total of 58 tumor tissues of neuroblastoma patients with clinical follow-up information and characteristics were acquired from Tianjin Medical University Cancer Institute and Hospital, from 2014 to 2020. This investigation was carried out in adherence to the guidelines delineated in the Declaration of Helsinki established by the World Medical Association. Furthermore, it was carried out with agreement from the Research Ethics Committee at Tianjin Medical University Cancer Institute and Hospital (Approval Code: EK2023115). Immunohistochemical (IHC) staining procedures were performed as follows: Histopathological Section (4μm thick) were subjected to an overnight incubation at 60 °C for baking, followed by a process of deparaffinization and subsequent dehydration. Subsequent steps included antigen retrieval and inhibition of endogenous peroxidase activity. Tissue sections were subsequently placed in a humidified chamber at 4 °C for 24 h with incubation of the primary anti-ABLIM3 antibody (dilution 1:100; Santa Cruz Biotechnology, California, USA). This step was succeeded by a 1-hour incubation at room temperature with the appropriate secondary antibodies. The reaction product was visualized by the addition of diaminobenzidine (DAB) for 5 min until a brown coloration appeared. Digital images were captured using Leica light microscopes. The immunostaining score for ABLIM3 was assessed by evaluating both the proportion of positively stained cells and the intensity of the staining. Based on the ABLIM3 immunoscore, NB patients were classified into three distinct categories: (Low expression: 0–3; Medium expression: 4–6; and High expression: 8–12).

2.12. Real-time qPCR

Real-time quantitative polymerase chain reaction (RT-qPCR) was employed for the assessment of gene expression levels. The extraction of total RNA from cell samples was conducted employing the TRIzol reagent. Following this extraction, the RNA obtained was then converted into complementary DNA (cDNA) through reverse transcription using the StarScript III RT kit (A232, GenStar, China). The RT-qPCR process was performed using the RealStar Power SYBR qPCR Mix (A311, GenStar, China), according to the manufacturer's instructions. The relative expression of target genes was normalized to the expression of a reference gene GAPDH to control for sample-to-sample variation. The $2^-\Delta\Delta Ct$ method was employed for data normalization and analysis. All qPCR reactions were performed in triplicate to ensure reproducibility and reliability of the results. The GAPDH was selected as reference gene. The primer sequences for the target gene were shown in Supplementary Table 6.

2.13. Western blotting

After transfecting ABLIM3 shRNAs into NB cells for 48 h, cells were collected and Total protein was extracted using Whole Cell Lysis Assay kits (Keygen Biotech, China). Subsequently, western blot analysis was conducted to assess the expression levels of the target protein. For details: Protein samples were loaded onto PVDF membranes, which were then blocked with 5 % non-fat milk to prevent nonspecific antibody binding. To block the nonspecific antibody binding, the PVDF membrane was incubated with 5 % non-fat milk for 2 h at room temperature. Then they were incubated at 4 ℃ overnight with specific antibodies: anti-ABLIM3 (1:1000, sc-398575, Santa Cruz Biotechnology, California, USA), ITGA3 (1:1000, A17502, Abclonal, Wuhan, China), ITGA8 (1:1000, A13056, Abclonal, Wuhan, China), KRT19 (1:1000, A0247, Abclonal, Wuhan, China), β-actin (1:5000, 66009–1-Ig, Proteintech, Wuhan, China) and anti-GADPH (1:1000, Proteintech, Wuhan, China,). Membranes were washed with $1 \times$ TBST 3 times (5 min/each time), and incubated with the appropriate horseradish peroxidase–conjugated goat anti-mouse antibodies (1:1000, Proteintech, Wuhan, China) for 1.5 h (room temperature). Then, the proteins were detected by the enhanced

chemiluminescence reagents (Thermo Scientific, USA).

2.14. Statistical analysis

All the statistical analyses were executed utilizing GraphPad Prism 8 and R software 4.1.3. Statistical findings within this study are delineated as mean $\pm$ standard deviation (mean $\pm$ SD). The appropriateness of statistical tests, including the Chi-square test and Student's t test, was determined based on the data under consideration. $P < 0.05$ was set to indicate statistical significance.

3. Results

3.1. Identifying Hub genes for neuroblastoma metastasis based on integrated machine learning algorithms

The GSE25624 dataset was sourced from the NCBI GEO database, which included 8 normal Adrenal glands, 9 localized NB tissues, and 29 distant metastasis tissues. Our research selected the localized NB tissues (n = 9), and distant metastasis tissues(n = 29) for further study. After consolidating these original data, the DEGs were explored by the "limma" package in R software. The threshold for DEGs was FDR < 0.05 and |logFC| $\geq$ 1. Consequently, 314 DEGs were identified, including 134 up-regulated and 180 down-regulated in the distant metastasis group (Fig. 1A, supplement Fig. 1A). GO and KEGG analysis was performed to further explore the potential biological function and molecular mechanisms of these DEGs, and the "clusterProfiler" package in R software (Version 4.13) was used. The results of GO analysis indicated that these DEGs mainly enriched in the biological processes including blood coagulation, response to type I interferon, and detoxification of inorganic compounds. For the cellular component, these DEGs were significantly enriched in the collagen-containing extracellular matrix, endoplasmic reticulum lumen, secretory granule lumen, and fibrillary collagen. As for the molecular function, we found these DEGs mainly enriched in receptor-ligand activity, extracellular matrix structural constituent, and CXCR chemokine receptor binding (Fig. 1B). The KEGG analysis showed that these DEGs mainly participated in the PI3K-AKT signaling pathway, Focal adhesion pathway, ECM receptor interaction, P53 signaling pathway, and TGF-β signaling pathway (Fig. 1C).

To further identify the hub biomarkers, three integrated machine-learning algorithms were conducted. The Lasso regression analysis showed that a total of 16 DEGs were identified from the 314 DEGs, which have the lowest binomial deviation (Fig. 1D, Supplementary Table 1). The SVM-RFE algorithm identified the 2 genes that had the highest accuracy and the lowest error (Fig. 1E, Supplementary Table 2). Then, the random forest was performed to identify the most important gene involved in the NB metastasis, and the importance score of these genes was calculated (Fig. 1F, Supplementary Table 3). The importance of these DEGs is shown in Supplement Fig. 1B. Finally, a Venn diagram was performed, and ABLIM3 was intersected (Fig. 1G).

3.2. Low expression of ABLIM3 was associated with adverse outcomes for NB patients

In investigating the association between ABLIM3 expression and clinical-pathologic characteristics of NB patients, we compared the expression of ABLIM3 between different groups and found that lower expression of ABLIM3 was associated with older age at diagnosis (Age $\geq$18 months, $P = 1.2$ e-11) (Fig. 2A). And, patients in INSS stages 1/2/3/4s showed higher ABLIM3 expression than those in INSS stage 4 (Fig. 2B, $P < 0.0021$). Patients in the high-risk group ($P < 2.22$e-16), accompanied by MYCN amplification ($P < 2.22$e-16) showed a lower ABLIM3 expression (Fig. 2C-D). NB patients with tumor progression also showed a lower ABLIM3 expression ($P < 2.22$e-16) (Fig. 2E). Besides, K-M survival analysis was conducted, and we found that patients with low expression showed a lower 5-year survival rate (91 % vs 62 %,

$P < 0.001$, Fig. 2F).

3.3. ABLIM3 downregulation in NB tissues correlates with adverse prognosis

To further explore the prognostic value of ABLIM3, 58 neuroblastoma tissues from our hospital were selected, and the ABLIM3 protein expression levels were detected by Immunohistochemistry, and the result showed that the expression of ABLIM3 was lower in patients with metastasis ($P = 0.0075$) (Fig. 3A-B). Patients with Stage 4 showed a lower expression of ABLIM3 than those in Stage 1/2/3/4 s ($P = 0.03$) (Fig. 3C). Besides, the analysis of the ABLIM3 expression and clinical-pathologic characteristics showed that ABLIM3 was associated with metastasis status ($P = 0.0099$), INSS Stage ($P = 0.0401$), and COG Risk ($P = 0.0143$) (Table 1). Furthermore, the Kaplan–Meier curves analysis showed that NB patients with lower expression of ABLIM3 exhibited a worse event-free survival (EFS) rate ($P = 0.031$) and overall survival (OS) rate ($P = 0.023$) (Fig. 3D-E). Finally, the univariate and multivariate Cox regression analyses were performed, same as the age at diagnosis ($P < 0.001$), MYCN status ($P < 0.001$), and INSS stages ($P < 0.001$) are known as independent prognostic factors for NB patients, ABLIM3 also can be an independent prognostic factor for NB patients (HR=0.792, CI=0.661–0.950, $P = 0.012$, supplement Fig. 2A-B). These findings suggested that low expression of ABLIM3 was associated with a worse prognosis and a higher rate of metastasis.

3.4. Low expression of ABLIM3 indicated a high risk for immune evasion of NB patients

NB is clinically considered to be a typical "cold tumor", showing an impressive immune microenvironment with low immunogenicity. To explore the influence of ABLIM3 on the immune microenvironment, the TME scores were analyzed using the "estimate" Packages in R software (Version 4.1.3). The results revealed that low expression of ABLIM3 was significantly associated with a lower stromal score, lower immune score, and lower ESTIMATE score, indicating an impressive microenvironment ($P < 0.01$, Fig. 4A). Furthermore, the "CIBERSORT" algorithm was conducted to investigate the relationship between ABLIM3 and immune cells. The results revealed that ABLIM3 was positively related to T cells CD4 memory resting (P = 0.001), Dendritic cell resting ($P < 0.001$), Eosinophils ($P = 0.031$), and Macrophage M1 (P = 0.009), but negatively related to NK cell resting ($P = 0.049$), Mast cells activated ($P = 0.009$), Dendritic cells active ($P = 0.006$), B cells memory ($P = 0.006$), Plasma cells ($P < 0.001$), and Neutrophils ($P < 0.001$) (Fig. 4B). Additionally, an investigation was conducted into the correlation between ABLIM3 expression and the immune cell composition within the tumor microenvironment (TME). The expression of ABLIM3 was positive related with T cells CD4 memory resting (R=0.15, $P = 0.001$), Macrophages M1(R=0.12, $P = 0.0093$), Dendritic cells (R=0.15, $P = 0.00096$), but negative related with Mast cells active (R=−0.12, $P = 0.0088$), Plasma cells (R=−0.19, $P = 3.3$e-05) and Neutrophils (R=−0.25, $P = 3.3$e-08) (Fig. 4C).

Subsequently, the TIDE analysis was performed to evaluate the benefit from immunotherapy, and the results showed that patients with low ABLIM3 expression showed a higher TIDE score in comparison to those with high ABLIM3 expression ($P < 0.001$, Fig. 4D). This indicated that NB patients with lower ABLIM3 expression might benefit little from the immunotherapy due to the increased likelihood of immune evasion. Additionally, the expression of ABLIM3 varied among B cells memory, plasma cells, M1 macrophages, and Neutrophils ($P < 0.001$, Fig. 4E). Further investigation into the relationship between ABLIM3 and immune cell biomarkers identified 19 immune checkpoints significantly associated with ABLIM3 expression, particularly for CD4^{+}T cells, CD8^{+}T cells, Dendritic cells, M1 macrophages, M2 macrophages, and Neutrophils ($P < 0.001$, Table 2, supplement Figs. 3–4). Finally, the relationship between ABLIM3 and the immune function was analyzed in depth,
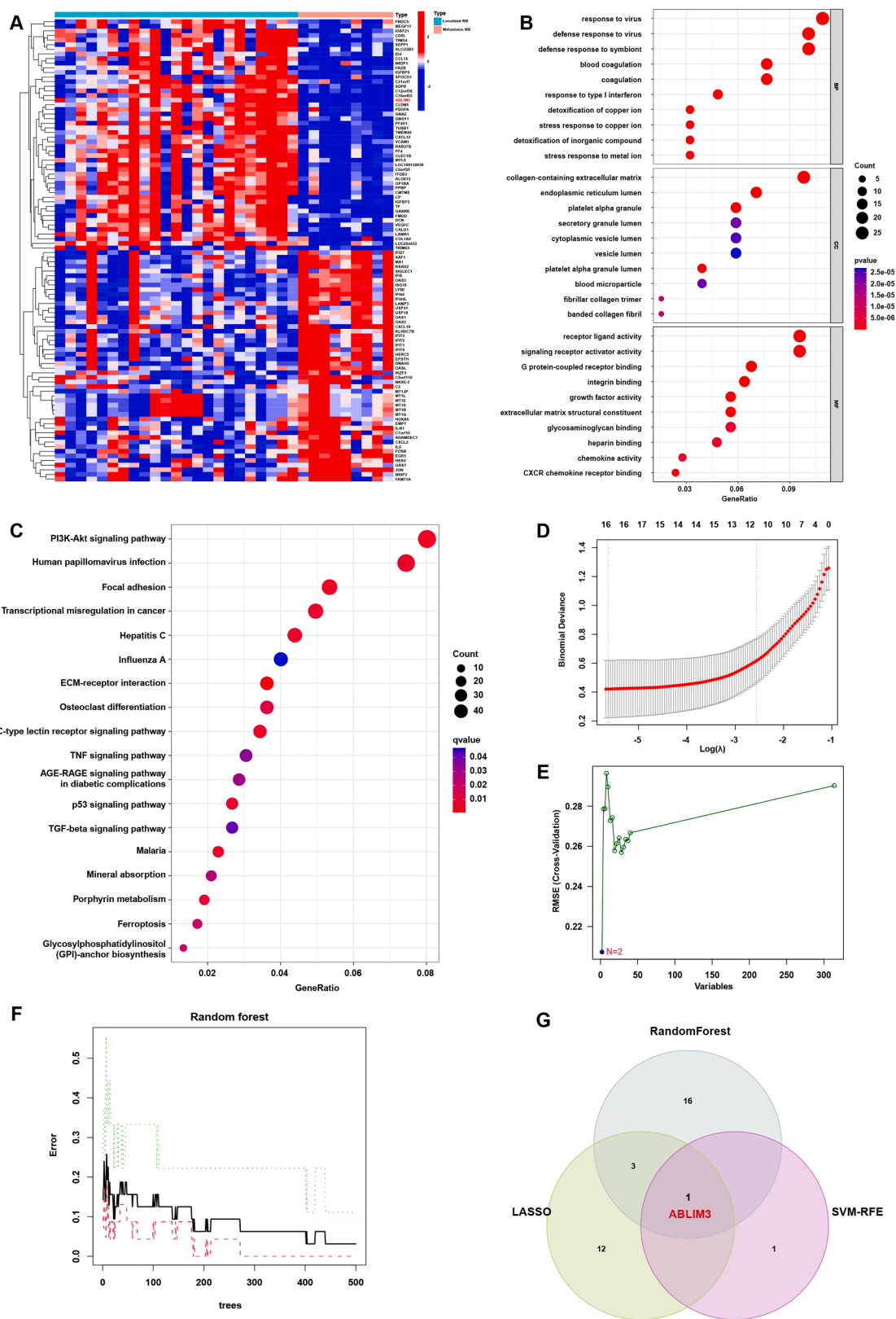
Fig. 1. Hub genes in the metastasis of neuroblastoma based on integrated machine learning algorithms. (A)The heatmap of differentially expressed genes between and local neuroblastoma and metastasis site; (B-C) Gene ontology (encompassing Biological Process (BP), Cellular Component (CC), and Molecular Function (MF) categories) and KEGG pathway enrichment analysis were conducted for these DEGs. (D) The Lasso regression analysis of the differentially expressed DEGs in NB; (E) The SM-RFE algorithm analysis for the differentially expressed DEGs in NB patients; (F) The random forest tree analysis for identifying the most important gene in the metastasis of NB patients; (G) The wenn diagram to identify the hub genes among LASSO aggression analysis, SVM-RFE, and the random forest tree algorithm.
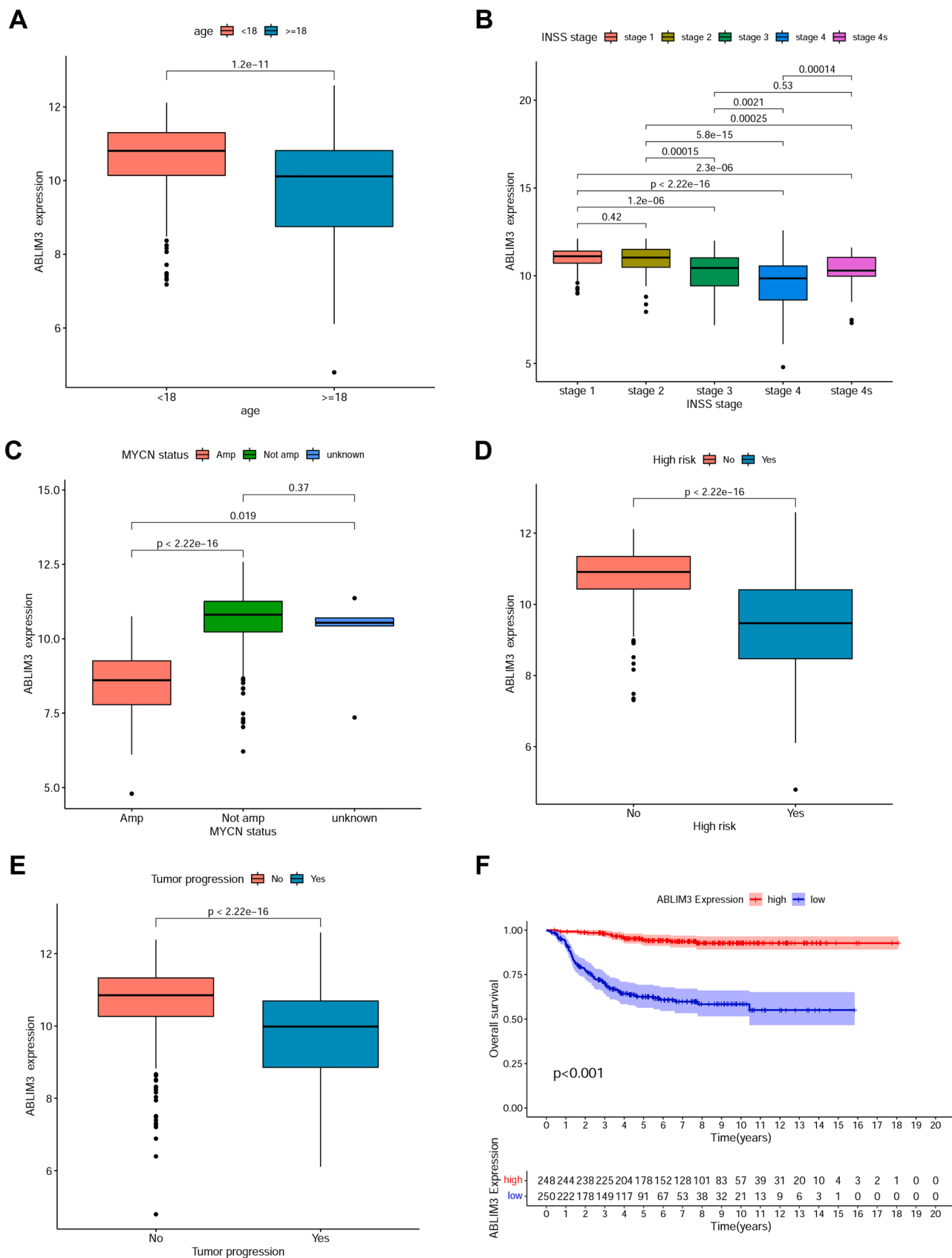
Fig. 2. Low expression of ABLIM3 was associated with poor prognosis for NB patients. (A) The different expression of ABLIM3 in the group between age < 18 months and age ≥ 18 months; (B) The expression of ABLIM3 among INSS stage1/2/3/4/4s; (C-E) The expression of ABLIM3 in the group of MYCN status, COG high-risk group, and NB patients with progression; (F) Kaplan–Meier curves of NB patients based on the expression of ABLIM3, and patients with low expression of ABLIM3 showed a better survival rate.

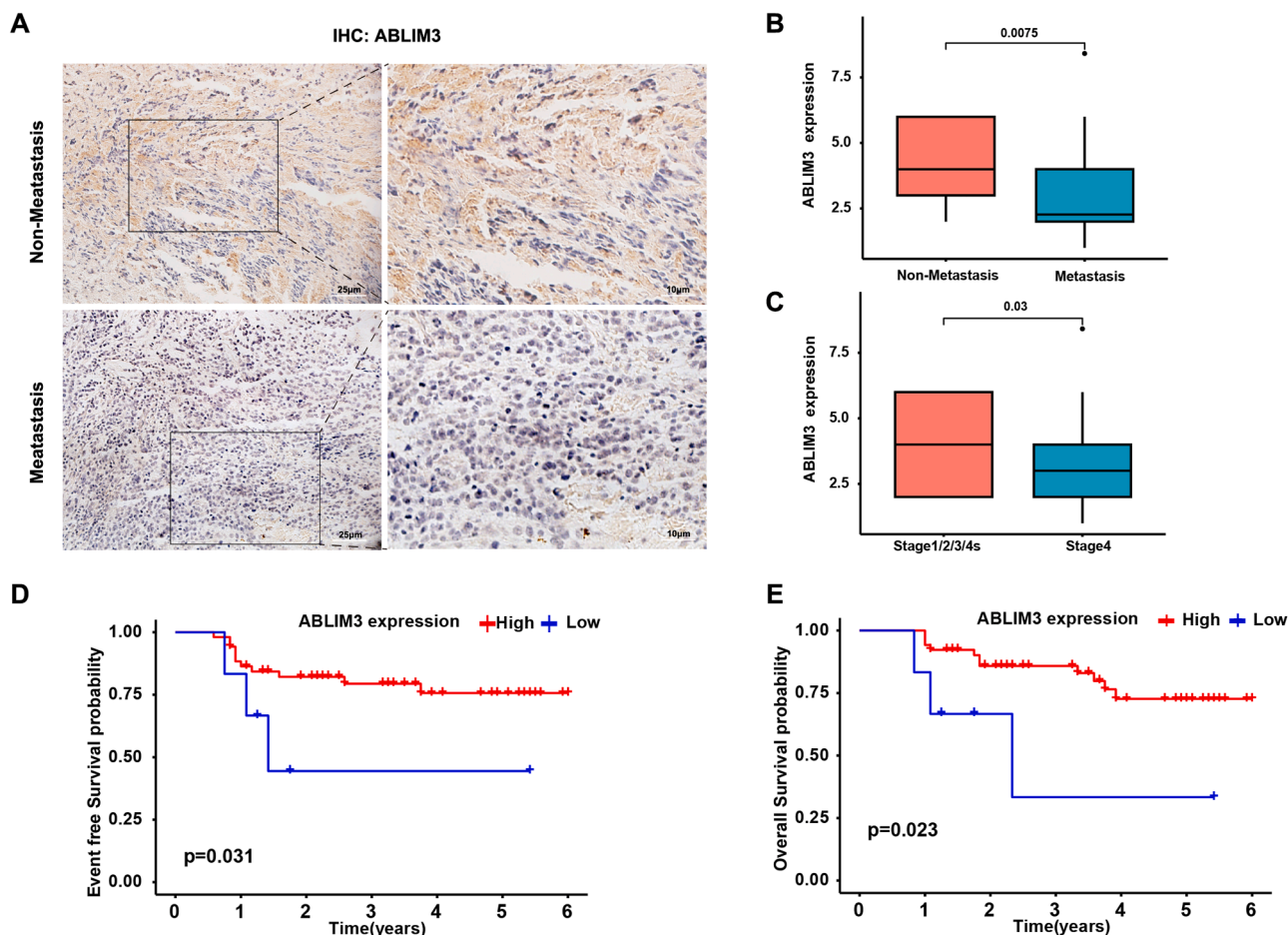**Fig. 3.** ABLIM3 downregulation in NB tissues correlates with adverse prognosis. (A) ABLIM3 was detected by IHC in NB tissues (Metastasis vs Non-Metastasis); (B) The expression of ABLIM3 between NB patients with/without metastasis (scale bar=25 μm or 10 μm); (C) The expression of ABLIM3 in INSS Stage1/2/3/4 s and INSS Stage4; (D-E) The Event-free survival rate and the overall survival rate of ABLIM3 in 58 NB patients (patients with high vs low expression of ABLIM3).

Table 1

Characteristics of Neuroblastoma patients and the association with ABLIM3 expression.

Characteristics	Group	Total	Low expression (n = 31)	High expression (n = 27)	chi	*P* value
Gender	Female	21(36.21 %)	12(38.71 %)	9(33.33 %)	0.0228	0.8799
	Male	37(63.79 %)	19(61.29 %)	18(66.67 %)		
Age	<18	19(32.76 %)	11(35.48 %)	8(29.63 %)	0.0374	0.8466
	> = 18	39(67.24 %)	20(64.52 %)	19(70.37 %)		
Metastasis	NO	23(39.66 %)	7(22.58 %)	16(59.26 %)	6.6527	**0.0099**
	YES	35(60.34 %)	24(77.42 %)	11(40.74 %)		
BM metastasis	NO	29(50 %)	13(41.94 %)	16(59.26 %)	1.1087	0.2924
	YES	29(50 %)	18(58.06 %)	11(40.74 %)		
INSS stage	Stage1/2/3/4s	25(43.1 %)	9(29.03 %)	16(59.26 %)	4.2145	**0.0401**
	Stage4	33(56.9 %)	22(70.97 %)	11(40.74 %)		
COG Risk	High	32(55.17 %)	19(61.29 %)	13(48.15 %)	8.4895	**0.0143**
	Low	16(27.59 %)	4(12.9 %)	12(44.44 %)		
	Middle	10(17.24 %)	8(25.81 %)	2(7.41 %)		
Recurrence	NO	39(70.91 %)	20(68.97 %)	19(73.08 %)	0.0014	0.9698
	YES	16(29.09 %)	9(31.03 %)	7(26.92 %)		

revealing that patients with low expression of ABLIM3 demonstrated lower aDCs levels, APC co-stimulation, HLA, inflammation-promoting, MHC class I, NK cells, and T cell co-stimulation, TIL, and Type I IFN response ($P < 0.00001$) (Fig. 4F). These findings collectively suggest that patients with lower ABLIM3 expression may exhibit impaired immune activity, and showed an increased likelihood for immune evasion, and ABLIM3 could potentially serve as an immunotherapeutic target.

3.5. Downregulation of ABLIM3 increased the migration and invasion capacity of NB cells

To investigate the biological roles of ABLIM3 in neuroblastoma, three ABLIM3 shRNAs (#1, #2, #3) were designed and transfected them into NB cells (SK-N-AS and SK-N-BE2 cells) for 48 h, all three shRNA segments effectively down-regulated the expression of ABLIM3, with ABLIM3 shRNA#2 demonstrating the most significant reduction
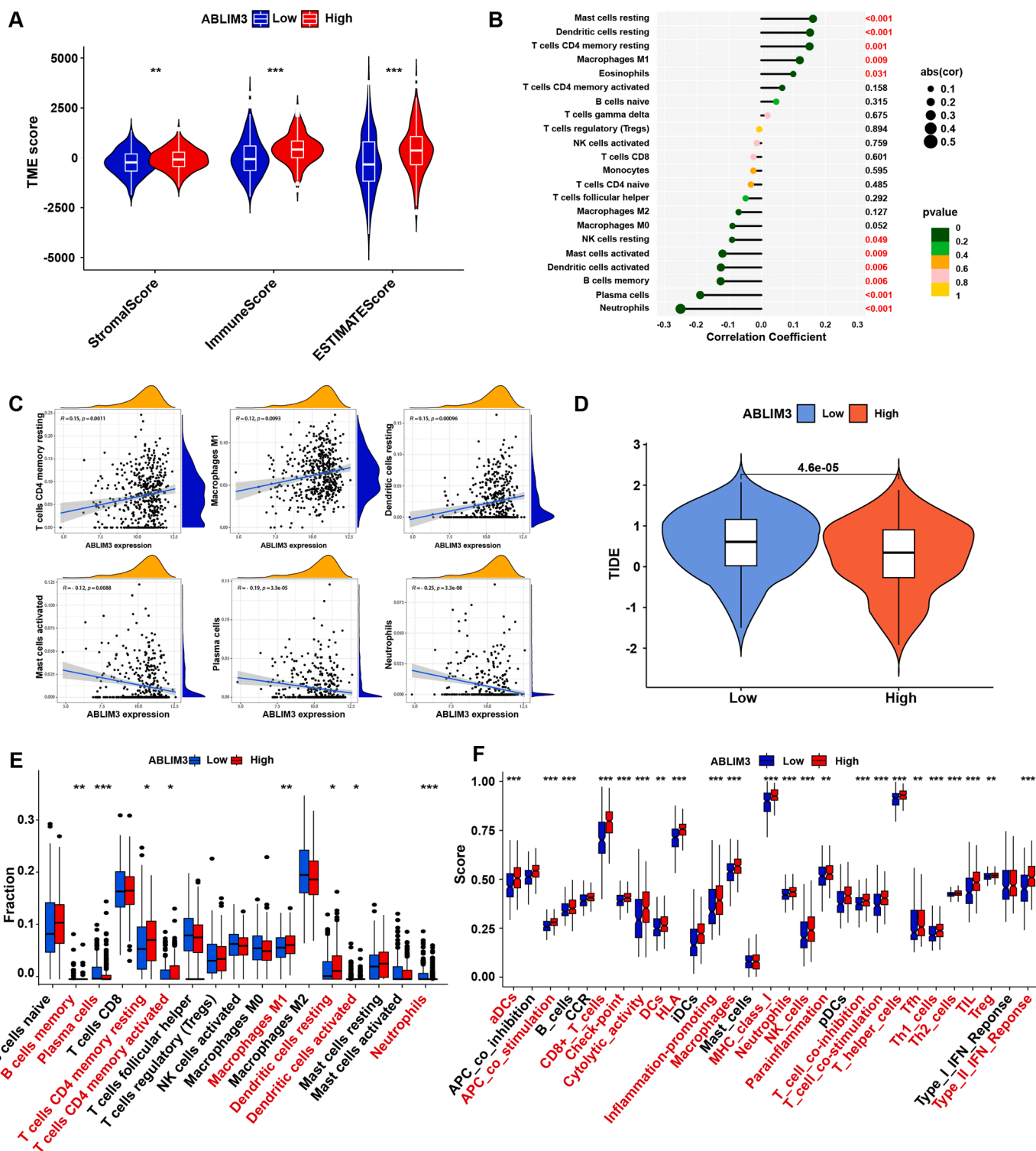
Fig. 4. Low expression ABLIM3 indicated an impressive immune microenvironment. (A) Comparative analysis of immune score, stromal score, and ESTIMATE Score, representing stromal cell presence within the tumor and tumor purity, across high and low ABLIM3 expression cohorts, ** $P < 0.01$, *** $P < 0.001$, ABLIM3 high expression versus ABLIM3 low expression groups.; (B-C) The correlation of ABLIM3 for immune cells in tumor microenvironment for NB; (D) The TIDE score between ABLIM3 high and low expression groups; (E) Differential expression of ABLIM3 across various immune cells between ABLIM3 high and low expression groups, ** $P < 0.01$, ** * $P < 0.001$; (F) The different immune function stage between ABLIM3 high and low expression group, * * $P < 0.01$, ** * $P < 0.001$.

(Fig. 5A-B). Subsequently, wound healing assays were performed to assess the influence of ABLIM3 on NB cell migration ability. The results revealed that the speed of scratch healing in NB cells transfected with ABLIM3 shRNA#2 was significantly faster than that in the control group (ctrl shRNA vs. ABLIM3 shRNA#2, In SK-N-AS cells: 17.66 % vs

56.96 %, $P < 0.001$; In SK-N-BE2 cells: 42.88 % vs 78.95 %, $P < 0.01$, Fig. 5C-D).

To further explore whether ABLIM3 influences the invasion ability of NB cells, SK-N-AS and SK-N-BE2 cells with or without ABLIM3 stably knockdown were seeded into the upper chambers of the Transwell

Table 2
The correlation between the expression of ABLIM3 and immune cells markers.

Immune cells	Gene	Cor	*P* value
B cell	CD19	0.16	0.000305862
	CD79A	0.06	1.78E-01
CD4⁺T cell	CD4	0.22	5.58E-07
CD8⁺T cell	CD8A	0.46	5.54E-27
	CD8B	0.26	7.24E-09
Dendritic cell	CD1C	0.47	3.48E-28
	HLA-DPA1	0.4	4.69E-20
	HLA-DPB1	0.42	4.02E-23
	HLA-DQB1	0.22	6.53E-07
	HLA-DRA	0.38	5.39E-19
	ITGAX	0.39	3.00E-19
	NRP1	0.45	9.89E-26
M1 macrophage	CD80	0.02	0.595420775
	CD86	-0.17	1.86E-04
	IRF5	0.1	0.020223345
	PTGS2	0.09	0.044491657
	CD32	-0.08	0.069198496
	CD16	-0.27	1.27E-09
M2 macrophage	CD163	0.18	7.19E-05
	CD206	0.22	1.11E-06
	MS4A4A	0.27	6.39E-10
	VSIG4	-0.16	0.000240162
Neutrophil	CCR7	0.36	1.93E-16
	CEACAM8	0.17	1.46E-04
	ITGAM	0.23	2.21E-07

inserts with Matrigel and incubated the lower chambers with 800ul RPMI-1640 medium (10 % FBS), 48 h later, the invading cell number was counted. There were more cells invaded into the lower chambers in NB cells transfected with ABLIM3 shRNA#2 than that in the control group (ctrl shRNA vs. ABLIM3 shRNA#2: 181.3 vs 375.8 in SK-N-AS cells, $P < 0.01$; 168.7 vs 309.0 in SK-N-BE2 cells, $P < 0.01$, Fig. 5E-F). Additionally, Phalloidin staining analysis demonstrated a significantly enhanced intensity of F-actin (green) in SK-N-AS and SK-N-BE2 cells transfected with ABLIM3 shRNA#2 when contrasted with the control group, indicating a greater invasive capacity ($P < 0.01$, Fig. 5G-H). These findings suggest that the ABLIM3 downregulation enhances the invasive and migratory potential of NB cells.

3.6. Downregulation of ABLIM3 promotes NB metastasis via regulating cell adhesion molecule ITGA3/ITGA8/KRT19

To further investigate the potential mechanism underlying ABLIM3′s influence the metastasis and the biological function in neuroblastoma, we divided NB samples (GSE49710, containing 498 samples) into two groups based on the median expression of ABLIM3. Differentially expressed analysis was performed by the "limma" package in R software (Version 4.1.3), and a total of 1740 DEGs were identified (Fig. 6A-B). The GO and KEGG signal pathway analyses revealed enrichment that the DEGs mainly enriched in T cell activation, lymphocyte-mediated immunity, positive regulation of cell-cell adhesion, MHC class II protein complex, and immune receptor activity for GO analysis. The KEGG pathway showed that DEGs mainly participate in cytokine-cytokine receptor interaction, cell adhesion molecules, Axon guidance, and the Th17 cell differentiation pathways (Fig. 6C-D). The GSEA analysis of genes related to ABLIM3 was conducted, and the results showed that those genes mainly enriched in Cell adhesion molecules and AXON guidance pathway (Fig. 6E). The Correlation analysis indicated that the expression of ABLIM3 was positively correlated with most of the metastasis-related biomarkers (supplement Fig. 4). Further investigation into potential mechanism of ABLIM3 in promoting NB metastasis, the genes enriched in the Cell adhesion molecules cams pathway were detected, the RT-PCR showed that the adhesion molecules including TWIST, ZEB1, CDH3, KRT19, ITGA3, and ITGA8 were downregulated in ABLIM3 shRNA transfected SK-N-AS cells (Fig. 6F), while only KRT19, ITGA3, and ITGA8 were downregulated in SK-N-BE2 cells (Fig. 6G).

Then, compared to the wild type and ctrl shRNA, the protein levels of KRT19, ITGA3, and ITGA8 were also downregulated in ABLIM3 shRNA transfected cells (Fig. 6H). These findings suggested that downregulation of ABLIM3 could promote metastasis by inhibiting the cell adhesion pathway, especially downregulating the expression of KRT19, ITGA3, and ITGA8.

3.7. Chemotherapeutic drugs identification for NB patients

To identify potential pharmacotherapeutic agents for neuroblastoma (NB) patients exhibiting distant metastasis, an inquiry into the GDSC database was conducted for the identification of prospective drugs. Integration of gene expression profiles and half-maximal inhibitory concentrations (IC50), it was discerned that individuals with elevated ABLIM3 expression manifested heightened sensitivity to a broad spectrum of chemotherapeutic agents. Conversely, those with diminished ABLIM3 expression displayed sensitivity exclusively to a limited subset of chemotherapeutic drugs, including Saracatinib, Erlotinib, Parthenolide, Embelin, Lisitinib, Bleomycin, Etoposide, and Tipifarnib (Fig. 7). Notably, despite the increased likelihood of metastasis observed in patients with reduced ABLIM3 expression, the aforementioned chemotherapeutic agents were identified as displaying promising therapeutic efficacy in addressing distant metastasis in NB patients.

4. Discussion

Neuroblastoma is the most common extra-vertebral solid tumor in children, and more than half of the patients are diagnosed with distant metastasis and fail to achieve a satisfactory response to treatment. In the current investigation, utilizing a combination of machine learning algorithms machine learning algorithms including LASSO regression, SVM-RFE, and random forest analysis, we identified ABLIM3 as a promising biomarker for metastasis in NB. Our findings suggest that ABLIM3 serves as an independent prognostic factor for NB patients, and low expression of ABLIM3 predicted a cold immune microenvironment and correlated with poor prognosis. Additionally, the downregulation of ABLIM3 promoted the migratory and invasive capabilities of NB cells via downregulating the expression of ITGA3, ITGA8 and KRT19, and inhibiting the metastasis-related pathway. Furthermore, our study identified potential pharmaceutical agents for the treatment of those patients with distant metastasis. These findings indicated that ABLIM3 may serve as a promising therapeutic target for NB patients with distant metastasis.

The LASSO regression analysis elegantly balances model simplicity with predictive precision, and the SVM-RFE analysis algorithm excels at pinpointing key genes to accurately predict metastasis. Additionally, the random forest tree analysis, an ensemble of decision trees, offers robust modeling for both prediction and elucidating disease mechanisms. Collectively, these methodologies have demonstrated exceptional efficacy in the identification of hub genes that participated in the metastasis of NB [31]. In this study, we identified ABLIM3 as the key regulator in the metastasis of NB patients, based on the three machine learning algorithms. Besides, patients with high expression of ABLIM3 showed a better prognosis than those with lower ABLIM3 expression. ABLIM3 was negatively correlated with age at diagnosis, INSS stages, MYCN status, and COG risk. Furthermore, we found that down-regulation of ABLIM3 could promote migration and invasion of NB cells. Miho et al. reported that ABLIM3 was a component of adherens junctions, and showed actin-binding activity in biological processes [11]. Adherens junctions dynamically modulate epithelial integrity through the restructuring of cell-to-cell adhesive interactions and were the basis of cancer cell metastasis [16,32]. In our study, GSEA analysis indicated that ABLIM3-associated genes mainly enriched in the metastasis pathway, such as the cell adhesion molecules (CAMs), and downregulation of ABLIM3 decreased the expression of cell adhesion molecules (ITGA3, ITGA8, and KRT19). The CAMs pathway play a vital role in the process
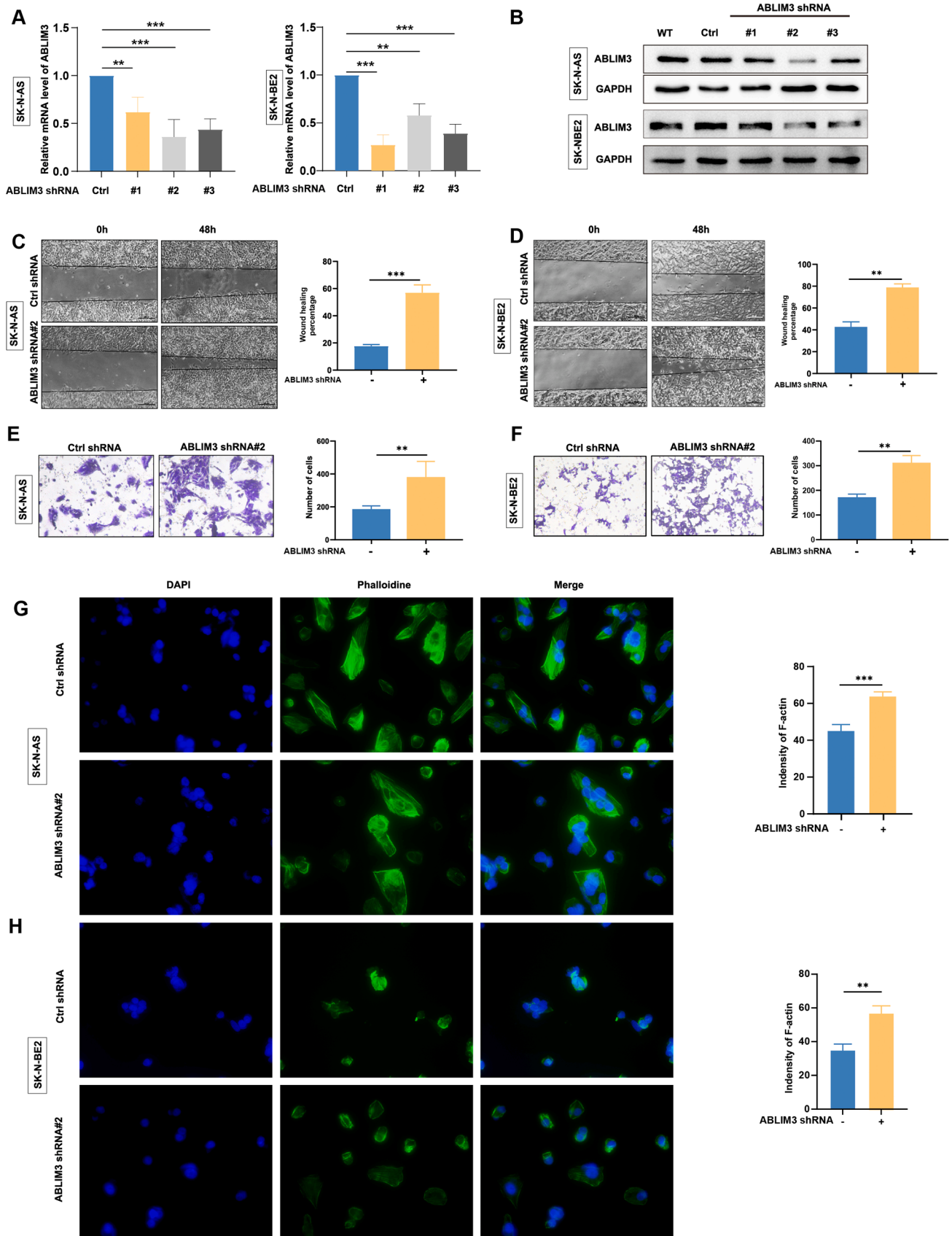
(caption on next page)

Fig. 5. Downregulation of ABLIM3 promoted cell migration and invasion of neuroblastoma cells. (A-B) SK-N-AS and SH-K-BE2 cells were transfected with ABLIM3 shRNAs (shRNA#1, #2, #3, and Ctrl shRNA) for 48 h, mRNA and protein were collected. Then, the expression of ABLIM3 was detected by RT-qPCR and Western blot; (C-D) 3×10^5 NB cells (SK-N-AS and SH-K-BE2) were seeded in 6-well plates after transfected with ABLIM3 shRNAs (shRNA#2 and Ctrl shRNA) and cultured for about 24 h (the cell density reached 100 %), cell scratch healing assay was performed to detected the cell migration (left), and the statistical analysis was conducted (right), ** $P < 0.01$, *** $P < 0.001$ control shRNA-transfected cells versus ABLIM3 shRNA#2-transfected cells, scale bar 100 μm; (E-F) 5×10^4 NB cells (SK-N-AS and SK-N-BE2) were seeded in trans-well insert (pretreated with Matrigel (30 μl, 1:7 diluted) after transfected with ABLIM3 shRNAs (Ctrl shRNA and shRNA#2), and the invasion assays were performed to evaluate the invasion ability (left), and the statistical analysis was conducted(right), ** $P < 0.01$, control shRNA-transfected cells versus ABLIM3 shRNA#2-transfected cells, scale size $100 \times$; (G) The Phalloidin fluorescent staining was used to visualize the F-actin (green) in NB cells, the nuclei (DAPI, blue) (left), the right was Quantitation of F-actin fluorescence intensity per area, scale bar $400 \times$ ** $P < 0.01$, *** $P < 0.01$.

of metastasis. ITGA3, ITGA8, and KRT19, as members of cell surface adhesion proteins, interact with extracellular matrix proteins and play a vital role in the process of tumor metastasis. Tang et al. found that ITGA3 mediated the lung metastasis of nasopharyngeal carcinoma [33]. ITGA3 was also found to regulate the metastasis of head and neck cancer [34], bladder cancer [35], and prostate cancer [36]. Ma et al. found that the hypermethylation of ITGA8 regulates the metastasis of bladder cancer [37]. Tang et al. found that Linc00974 interacts with KRT19 to promote the metastasis of hepatocellular cancer by activating the Notch and TGF-beta pathway [38]. Our research reveals that the down-regulation of ABLIME leads to decreased expression of ITGA3, ITGA8, and KRT19 at both mRNA and protein levels. Taken together, our findings suggest that ABLIM3 may promote the metastasis of NB cells via regulating cell adhesion molecules pathway, which expanded the mechanism of ABLIM3.

Fetahu et.al conducted a comprehensive analysis of bone marrow (BM) aspirates for 3 major NB subtypes and 5 NB patients without BM metastasis, utilizing single-cell transcriptomic and epigenetic profiling. They found that macrophages and migration inhibitory factors influence the BM microenvironment and inhibit the metastasis for NB cells, elucidating the relationship between tumor-to-microenvironment interactions [39]. High-risk NB patients exhibit a tumor microenvironment (TME) infiltrated by various immune cells, such as tumor-associated macrophages, NK cells, and myeloid-derived suppressor cells (MDSC) [3]. M2 tumor-associated macrophages (TAMs) are known to dampen immune responses and are associated with a sparse infiltration of tumor-related lymphocytes, a characteristic often referred to as a "cold tumor" in immunology. In our study, we found that the expression of ABLIM3 was positively correlated with macrophage M1, suggesting that ABLIM3 may promote NB metastasis by enhancing the aggression of macrophage M1. Additionally, ABLIM3 expression was found to be positively associated with mast cells, dendritic cells, CD4$^+$T cells, and Eosinophils. M1 macrophages have been reported to inhibit the proliferation and metastasis of NB cells [40]. Mast cells have been found to influence the remodeling of TME and tumor cell fate [41], and have been also reported to impair melanoma cell metastasis via decreasing the secretion of HMGA1 [42]. Dendritic cells, serving as antigen-presenting cells, can promote the infiltration of T cells into lung metastases and improve the efficacy of immunotherapies [43]. While, research on the role of ABLIM3 in influencing NB metastasis through the tumor microenvironment (TME) remains sparse.

Despite significant advancements in neuroblastoma (NB) treatment, a subset of patients, particularly those with metastatic disease, exhibit resistance to therapy [44]. Based on the drug sensitivity analysis, we found that many chemotherapeutic drugs were sensitive to patients with high ABLIM3 expression, while only a few drugs were suitable for patients with low expression of ABLIM3. Saracatinib, a selective Src kinase inhibitor, combat the metastases of head and neck cancer cells, and reduce the cancer-induced bone pain caused by bone metastasis [45,46]. Bone marrow is the most common site for NB cell metastasis, Saracatinib inhibits the cell proliferation of NB [47], indicating Saracatinib can be a candidate therapeutic drug for NB patients with metastasis. Etoposide was reported to form a complex with DNA and the topoisomerase II enzyme and inhibit the metastasis for cancer cells, showing high potential in the treatment of patients with neuroblastoma [48]. Erlotinib, a tyrosine kinase inhibitor, was found to block the kinase activity of EGFR

and showed promising antitumor potential for non-small cell lung cancer via FOXO3A/FOXM1 axis and IL-6/STAT3 signaling in vivo and in vitro [49,50]. Bleomycin showed promising anticancer potential for the metastasis of melanoma [51]. Bernstein et al. found Bleomycin showed cytotoxic action on neuroblastoma cells and inhibited the metastasis of NB patients [52]. Besides, Tipifarnib, a farnesyl transferase inhibitor targeting the HRAS oncogene, showed promising effectiveness in treating metastatic patients [53]. Liu et al. found that Tipifarnib inhibits small extracellular vesicle secretion, boosting the effectiveness of the GD2 monoclonal antibody (dinutuximab) immunotherapy in high-risk NB patients [54]. Further research on these drugs could enhance treatment selection for metastatic neuroblastoma, particularly for patients with low ABLIM3 expression, by identifying sensitive chemotherapeutic or targeted therapies.

Overall, our study indicates ABLIM3 as a promising therapeutic target for NB patients with metastasis. However, there were still several limitations in this study. Firstly, the influence of ABLIM3 on metastasis was only validated in NB cells, further experiment in vivo is needed. Additionally, our investigation only addressed that downregulation of ABLMI3 promotes the migration and invasion of NB cells, the effects of ABLIM3 overexpression remain unexplored. Moreover, the mechanism of ABLIM3 promotes the migration and invasion of NB cells, and the potential therapeutic drugs for patients with low expression of ABLIM3 still need to be explored.

In summary, ABLIM3 can act as an independent prognostic factor for NB patients, which showed a satisfactory ability to predict the prognosis for NB patients in the clinic. Knockdown the expression of ABLIM3 promoted the migration and invasion of NB by downregulating the expression of ITGA3, ITGA8, and KRT19. These suggest that ABLIM3 could be a potential therapeutic target for NB patients with metastasis.

Funding

CRediT authorship contribution statement

Jiaxing Yang: Investigation, Visualization, Writing – review & editing. **Chaoyu Wang:** Data curation, Methodology, Validation. **Yun Liu:** Investigation, Visualization, Writing – review & editing. **Yan Jin:** Project administration, Supervision. **Wenfeng Cao:** Project administration, Supervision. **Qiang Zhao:** Funding acquisition, Writing – review & editing. **Baocheng Gong:** Formal analysis, Software, Writing – original draft, Conceptualization. **Tongyuan Qu:** Conceptualization, Methodology, Software, Data curation. **Jiaojiao Zhang:** Data curation, Methodology. **Yubin Jia:** Investigation, Visualization, Writing – review & editing. **Chong Chen:** Investigation, Visualization, Writing – review & editing. **Zian Song:** Data curation, Methodology, Validation.

Consent to participate

All individuals were informed about the purposes of the study and signed their consent for publishing this research.
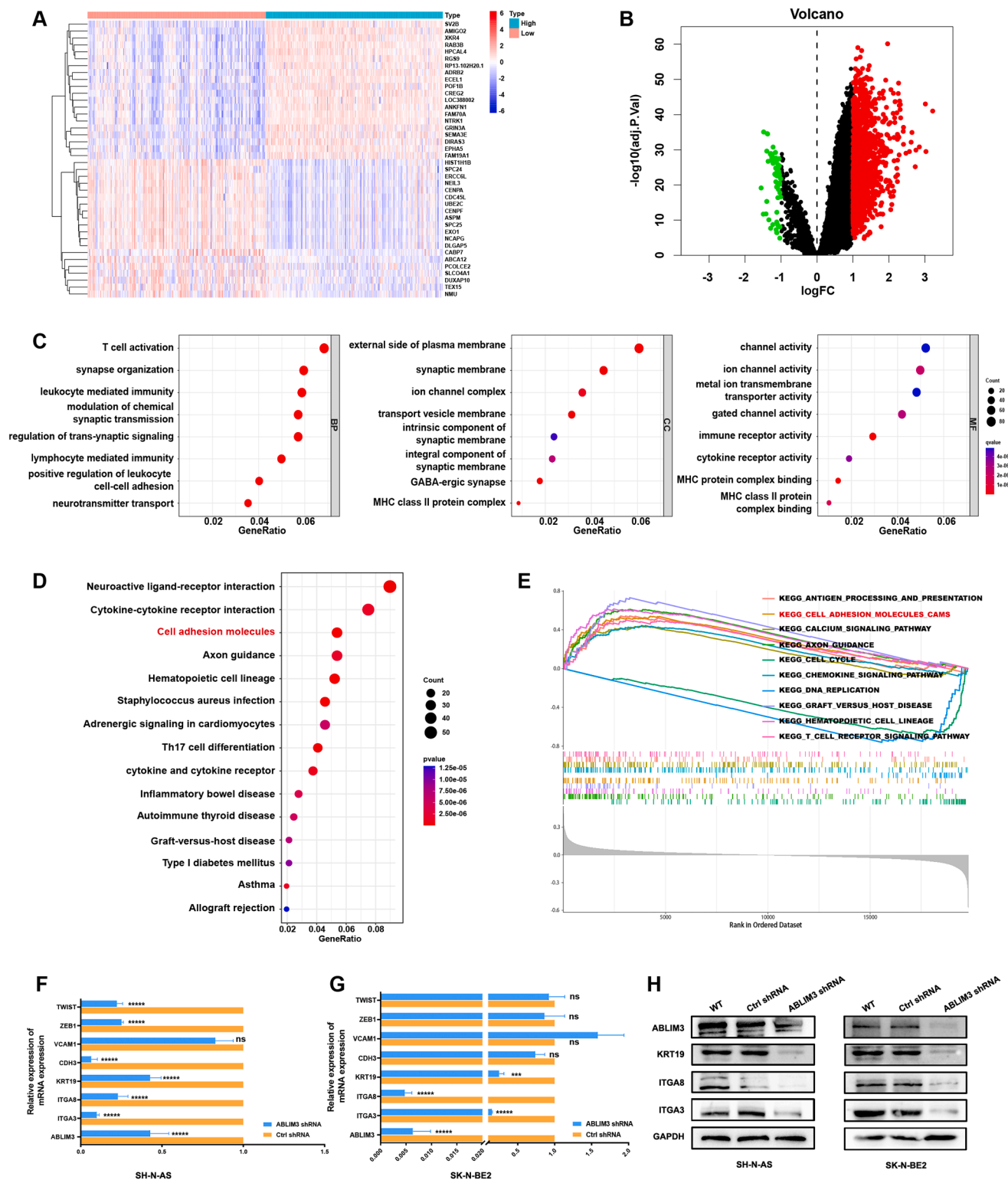
Fig. 6. Downregulation of ABLIM3 promotes NB metastasis via downregulating the expression of ITGA3/ITGA8/KRT19. (A) The heatmap of the top 20 differentially expressed genes, as determined by the median expression levels of ABLIM3 in GSE49710 (including 498 NB samples). Upregulated genes are denoted in red, while downregulated genes are indicated in blue; (B) The Volcano plot displays the distribution of differentially expressed genes, with red indicating upregulation, green indicating downregulation, and black indicating genes that did not show significant changes in expression levels (C-D) Enrichment analysis of Gene Ontology (GO) terms, encompassing Biological Process (BP), Cellular Component (CC), and Molecular Function (MF) categories, as well as Kyoto Encyclopedia of Genes and Genomes (KEGG) pathways, were conducted for the differentially expressed genes; (E) The GSEA pathway analysis between ABLIM3 high expression and ABLIM3 low expression groups; (F, G) The mRNA expression levels of genes enriched in the Cell Adhesion Molecules (CAMs) pathway were assessed in SK-N-AS and SK-N-BE2 cells using RT-qPCR following transfection with ABLIM3 shRNAs (Ctrl shRNA and shRNA#2) for 24 h, *** $P < 0.001$, **** $P < 0.0001$ control shRNA-transfected cells versus ABLIM3 siRNA#2-transfected cells; (H) Western blot analysis was performed to detect the protein expression levels of ITGA3, ITGA8, and KRT19 in neuroblastoma cells (SK-N-AS and SK-N-BE2) following transfection with ABLIM3 shRNAs (Ctrl shRNA and shRNA#2) for 48 h.
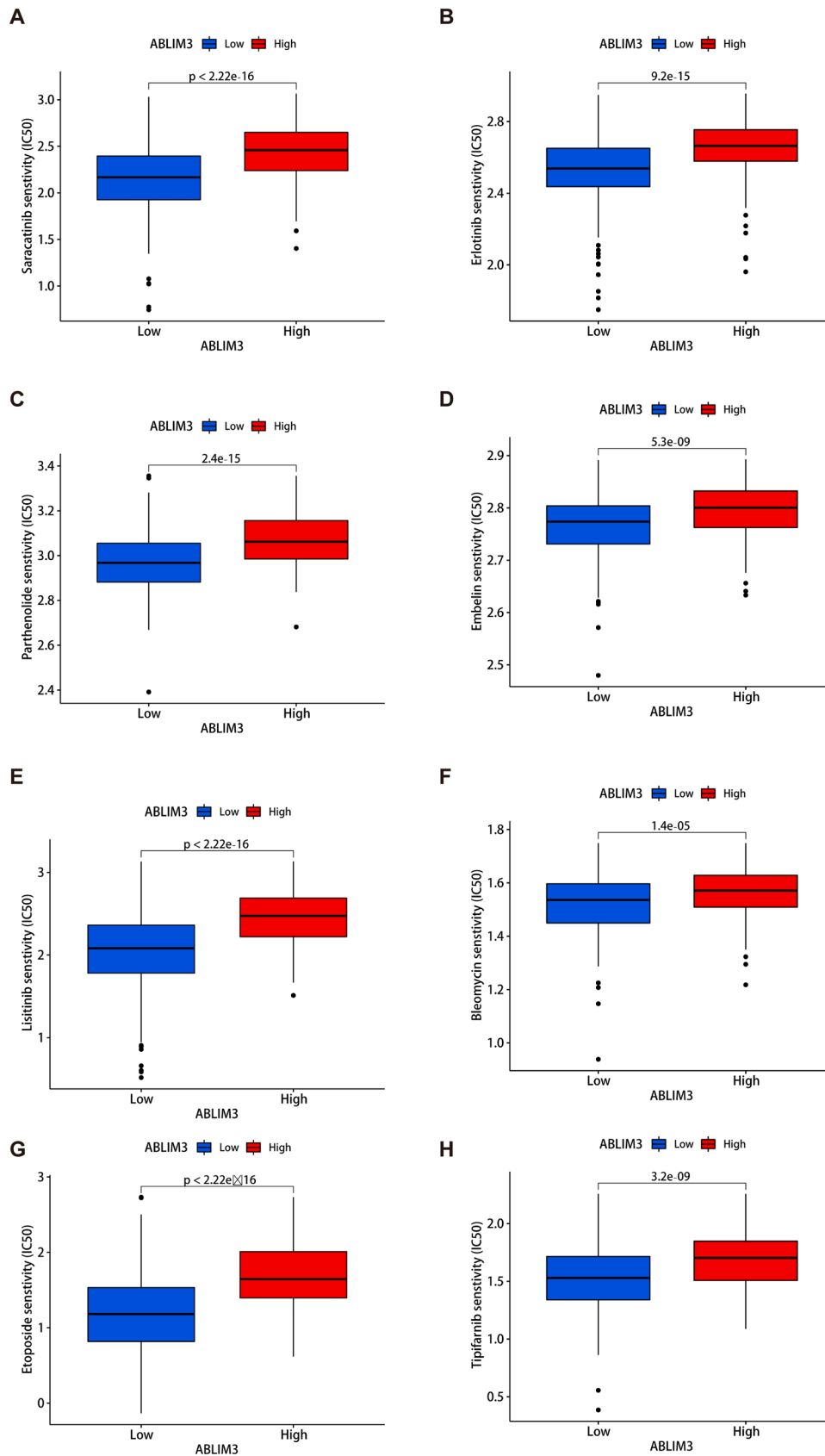
Fig. 7. Chemotherapeutic drugs identification for neuroblastoma patients. (A-H) Eight potential chemotherapeutic agents demonstrated significant efficacy in the treatment of NB patients exhibiting decreased ABLIM3 expression, with observed disparities in the IC50 values for various drugs between cases of high ABLIM3 expression and low ABLIM3 expression. These agents include Saracatinib (A), Erlotinib (B), Parthenolide (C), Embelin (D), Lisitinib (E), Bleomycin (F), Etoposide (G), and Tipifarnib (H).

Consent for publication

All authors agreed with its publication in the current form.

Code availability

The "Materials and methods" section includes all analysis methods, software packages, and online tools. The code used in this study is available from the corresponding author upon reasonable request.

Declaration of Competing Interest

1. All individuals were informed about the purposes of the study and signed their consent for publishing this research.
2. There are no conflicts of interest to disclose for this paper.

Data availability

The data supporting the conclusions of this article are available in the article, Supplementary material, and the GEO database(https://www.ncbi.nlm.nih.gov/geo/). Further inquiries are available from the corresponding authors on a reasonable request.

Acknowledgments

Appendix A. Supporting information

Supplementary data associated with this article can be found in the online version at doi:10.1016/j.csbj.2024.04.024.

References

[1] Ponzoni M, Bachetti T, Corrias MV, Brignole C, Pastorino F, Calarco E, et al. Recent advances in the developmental origin of neuroblastoma: an overview. J Exp Clin Cancer Res: CR 2022;41(1):92.

[2] Maris JM. Recent advances in neuroblastoma. N Engl J Med 2010;362(23):2202–11.

[3] Qiu B, Matthay KK. Advancing therapy for neuroblastoma. Nat Rev Clin Oncol 2022;19(8):515–33.

[4] Brodeur GM. Neuroblastoma: biological insights into a clinical enigma. Nat Rev Cancer 2003;3(3):203–16.

[5] Fletcher JI, Ziegler DS, Trahair TN, Marshall GM, Haber M, Norris MD. Too many targets, not enough patients: rethinking neuroblastoma clinical trials. Nat Rev Cancer 2018;18(6):389–400.

[6] Butler E, Ludwig K, Pacenta HL, Klesse LJ, Watt TC, Laetsch TW. Recent progress in the treatment of cancer in children, CA: a cancer. J Clin 2021;71(4):315–32.

[7] Haug CJ, Drazen JM. Artificial intelligence and machine learning in clinical medicine, 2023. N Engl J Med 2023;388(13):1201–8.

[8] You Y, Lai X, Pan Y, Zheng H, Vera J, Liu S, et al. Artificial intelligence in cancer target identification and drug discovery. Signal Transduct Target Ther 2022;7(1):156.

[9] Cammarota G, Ianiro G, Ahern A, Carbone C, Temko A, Claesson MJ, et al. Gut microbiome, big data and machine learning to promote precision medicine for cancer, Nature reviews. Gastroenterol Hepatol 2020;17(10):635–48.

[10] Swanson K, Wu E, Zhang A, Alizadeh AA, Zou J. From patterns to patients: advances in clinical machine learning for cancer diagnosis, prognosis, and treatment. Cell 2023;186(8):1772–91.

[11] Matsuda M, Yamashita JK, Tsukita S, Furuse M. abLIM3 is a novel component of adherens junctions with actin-binding activity. Eur J Cell Biol 2010;89(11):807–16.

[12] Liu D, Wang X, Liu Y, Li C, Zhang Z, Lv P. Actin-binding LIM 1 (ABLIM1) inhibits glioblastoma progression and serves as a novel prognostic biomarker. Dis Markers 2022 2022:9516808.

[13] Dong X, Feng M, Yang H, Liu H, Guo H, Gao X, et al. Rictor promotes cell migration and actin polymerization through regulating ABLIM1 phosphorylation in Hepatocellular Carcinoma. Int J Biol Sci 2020;16(15):2835–52.

[14] Elagib KE, Brock A, Clementelli CM, Mosoyan G, Delehanty LL, Sahu RK, et al. Relieving DYRK1A repression of MKL1 confers an adult-like phenotype to human infantile megakaryocytes. J Clin Investig 2022;132(19).

[15] Krupp M, Weinmann A, Galle PR, Teufel A. Actin binding LIM protein 3 (abLIM3). Int J Mol Med 2006;17(1):129–33.

[16] Law RA, Kiepas A, Desta HE, Perez Ipiña E, Parlani M, Lee SJ, et al. Cytokinesis machinery promotes cell dissociation from collectively migrating strands in confinement. Sci Adv 2023;9(2):eabq6480.

[17] Wei M, Ma Y, Shen L, Xu Y, Liu L, Bu X, et al. NDRG2 regulates adherens junction integrity to restrict colitis and tumourigenesis. EBioMedicine 2020;61:103068.

[18] Sacks D, Baxter B, Campbell BCV, Carpenter JS, Cognard C, Dippel D, et al. Multisociety consensus quality improvement revised consensus statement for endovascular therapy of acute ischemic stroke. Int J Stroke Off J Int Stroke Soc 2018;13(6):612–32.

[19] Wells A, Grahovac J, Wheeler S, Ma B, Lauffenburger D. Targeting tumor cell motility as a strategy against invasion and metastasis. Trends Pharmacol Sci 2013;34(5):283–9.

[20] Lin W, Fang J, Wei S, He G, Liu J, Li X, et al. Extracellular vesicle-cell adhesion molecules in tumours: biofunctions and clinical applications. Cell Commun Signal: CCS 2023;21(1):246.

[21] Santarosa M, Maestro R. The autophagic route of E-cadherin and cell adhesion molecules in cancer progression. Cancers 2021;13(24).

[22] Li M, Wang Y, Li M, Wu X, Setrerrahmane S, Xu H. Integrins as attractive targets for cancer therapeutics. Acta Pharm Sin B 2021;11(9):2726–37.

[23] Fuchs BC, Bode BP. Amino acid transporters ASCT2 and LAT1 in cancer: partners in crime. Semin Cancer Biol 2005;15(4):254–66.

[24] Ritchie ME, Phipson B, Wu D, Hu Y, Law CW, Shi W, et al. limma powers differential expression analyses for RNA-sequencing and microarray studies. Nucleic Acids Res 2015;43(7):e47.

[25] Wu T, Hu E, Xu S, Chen M, Guo P, Dai Z, et al. clusterProfiler 4.0: a universal enrichment tool for interpreting omics data. Innov (Camb (Mass)) 2021;2(3):100141.

[26] Tibshirani R. Regression shrinkage and selection via the lasso: a retrospective. J R Stat Soc Ser B: Stat Methodol 2011;73(3):273–82.

[27] Huang ML, Hung YH, Lee WM, Li RK, Jiang BR. SVM-RFE based feature selection and Taguchi parameters optimization for multiclass SVM classifier. TheScientificWorldJournal 2014;2014:795624.

[28] Blanchet L, Vitale R, van Vorstenbosch R, Stavropoulos G, Pender J, Jonkers D, et al. Constructing bi-plots for random forest: tutorial. Anal Chim Acta 2020;1131:146–55.

[29] Newman AM, Liu CL, Green MR, Gentles AJ, Feng W, Xu Y, et al. Robust enumeration of cell subsets from tissue expression profiles. Nat Methods 2015;12(5):453–7.

[30] Yang W, Soares J, Greninger P, Edelman EJ, Lightfoot H, Forbes S, et al. Genomics of drug sensitivity in cancer (GDSC): a resource for therapeutic biomarker discovery in cancer cells. Nucleic Acids Res 2013;41(Database issue):D955–61.

[31] Sanz H, Valim C, Vegas E, Oller JM, Reverter F. SVM-RFE: selection and visualization of the most relevant features through non-linear kernels. BMC Bioinforma 2018;19(1):432.

[32] Kato T, Jenkins RP, Derzsi S, Tozluoglu M, Rullan A, Hooper S, et al. Interplay of adherens junctions and matrix proteolysis determines the invasive pattern and growth of squamous cell carcinoma. eLife 2023;12.

[33] Tang XR, Wen X, He QM, Li YQ, Ren XY, Yang XJ, et al. MicroRNA-101 inhibits invasion and angiogenesis through targeting ITGA3 and its systemic delivery inhibits lung metastasis in nasopharyngeal carcinoma. Cell death Dis 2017;8(1):e2566.

[34] Koshizuka K, Hanazawa T, Kikkawa N, Arai T, Okato A, Kurozumi A, et al. Regulation of ITGA3 by the anti-tumor miR-199 family inhibits cancer cell migration and invasion in head and neck cancer. Cancer Sci 2017;108(8):1681–92.

[35] Wang JR, Liu B, Zhou L, Huang YX. MicroRNA-124-3p suppresses cell migration and invasion by targeting ITGA3 signaling in bladder cancer, cancer biomarkers: section. A Dis Markers 2019;24(2):159–72.

[36] Kurozumi A, Goto Y, Matsushita R, Fukumoto I, Kato M, Nishikawa R, et al. Tumor-suppressive microRNA-223 inhibits cancer cell migration and invasion by targeting ITGA3/ITGB1 signaling in prostate cancer. Cancer Sci 2016;107(1):84–94.

[37] Ma X, Zhang L, Liu L, Ruan D, Wang C. Hypermethylated ITGA8 facilitate bladder cancer cell proliferation and metastasis. Appl Biochem Biotechnol 2023.

[38] Tang J, Zhuo H, Zhang X, Jiang R, Ji J, Deng L, et al. A novel biomarker Linc00974 interacting with KRT19 promotes proliferation and metastasis in hepatocellular carcinoma. Cell death Dis 2014;5(12):e1549.

[39] Fetahu IS, Esser-Skala W, Dnyansagar R, Sindelar S, Rifatbegovic F, Bileck A, et al. Single-cell transcriptomics and epigenomics unravel the role of monocytes in neuroblastoma bone marrow metastasis. Nat Commun 2023;14(1):3620.

[40] Relation T, Yi T, Guess AJ, La Perle K, Otsuru S, Hasgur S, et al. Intratumoral delivery of interferonγ-secreting mesenchymal stromal cells repolarizes tumor-associated macrophages and suppresses neuroblastoma proliferation in vivo. Stem Cells 2018;36(6):915–24.

[41] Shi S, Ye L, Yu X, Jin K, Wu W. Focus on mast cells in the tumor microenvironment: current knowledge and future directions. Biochim Et Biophys Acta Rev Cancer 2023;1878(1):188845.

[42] Benito-Martin A, Nogués L, Hergueta-Redondo M, Castellano-Sanz E, Garvin E, Cioffi M, et al. Mast cells impair melanoma cell homing and metastasis by inhibiting HMGA1 secretion. Immunology 2023;168(2):362–73.

[43] Chiang MR, Shen WT, Huang PX, Wang KL, Weng WH, Chang CW, et al. Programmed T cells infiltration into lung metastases with harnessing dendritic cells in cancer immunotherapies by catalytic antigen-capture sponges. J Control Release: J Control Release Soc 2023;360:260–73.

[44] DuBois SG, Granger MM, Groshen S, Tsao-Wei D, Ji L, Shamirian A, et al. Randomized phase II trial of MIBG versus MIBG, vincristine, and irinotecan versus

mibg and vorinostat for patients with relapsed or refractory neuroblastoma: a report from NANT consortium. J Clin Oncol 2021;39(31):3506–14.

[45] Lang L, Shay C, Xiong Y, Thakkar P, Chemmalakuzhy R, Wang X, et al. Combating head and neck cancer metastases by targeting Src using multifunctional nanoparticle-based saracatinib. J Hematol Oncol 2018;11(1):85.

[46] Danson S, Mulvey MR, Turner L, Horsman J, Escott K, Coleman RE, et al. An exploratory randomized-controlled trial of the efficacy of the Src-kinase inhibitor saracatinib as a novel analgesic for cancer-induced bone pain. J Bone Oncol 2019; 19:100261.

[47] Yadikar H, Torres I, Aiello G, Kurup M, Yang Z, Lin F, et al. Screening of tau protein kinase inhibitors in a tauopathy-relevant cell-based model of tau hyperphosphorylation and oligomerization. PLoS One 2020;15(7):e0224952.

[48] Ladenstein R, Pötschger U, Pearson ADJ, Brock P, Luksch R, Castel V, et al. Busulfan and melphalan versus carboplatin, etoposide, and melphalan as high-dose chemotherapy for high-risk neuroblastoma (HR-NBL1/SIOPEN): an international, randomised, multi-arm, open-label, phase 3 trial. Lancet Oncol 2017;18(4): 500–14.

[49] Li J, Chen P, Wu Q, Guo L, Leong KW, Chan KI, et al. A novel combination treatment of antiADAM17 antibody and erlotinib to overcome acquired drug resistance in non-small cell lung cancer through the FOXO3a/FOXM1 axis. Cell Mol Life Sci 2022;79(12):614.

[50] Tang CH, Qin L, Gao YC, Chen TY, Xu K, Liu T, et al. APE1 shRNA-loaded cancer stem cell-derived extracellular vesicles reverse erlotinib resistance in non-small cell lung cancer via the IL-6/STAT3 signalling. Clin Transl Med 2022;12(5):e876.

[51] Kivelä T, Suciu S, Hansson J, Kruit WH, Vuoristo MS, Kloke O, et al. Bleomycin, vincristine, lomustine and dacarbazine (BOLD) in combination with recombinant interferon alpha-2b for metastatic uveal melanoma. Eur J Cancer 2003;39(8): 1115–20.

[52] Polavarapu S, Mani AM, Gundala NK, Hari AD, Bathina S, Das UN. Effect of polyunsaturated fatty acids and their metabolites on bleomycin-induced cytotoxic action on human neuroblastoma cells in vitro. PLoS One 2014;9(12):e114766.

[53] Ho AL, Brana I, Haddad R, Bauman J, Bible K, Oosting S, et al. Tipifarnib in head and neck squamous cell carcinoma with HRAS mutations. J Clin Oncol 2021;39 (17):1856–64.

[54] Liu X, Wills CA, Chen L, Zhang J, Zhao Y, Zhou M, et al. Small extracellular vesicles induce resistance to anti-GD2 immunotherapy unveiling tipifarnib as an adjunct to neuroblastoma immunotherapy. J Immunother Cancer 2022;10(4).